Journal of Liposome Research, 16:57–80, 2006

ISSN: 0898-2104
DOI: 10.1080/08982100500528842

Reducing Liposome Size with Ultrasound: Bimodal Size Distributions

DIXON J. WOODBURY, ERIC S. RICHARDSON, AARON W. GRIGG, RODNEY D. WELLING, AND BRIAN H. KNUDSON

Department of Physiology and Developmental Biology, Brigham Young University, Provo, UT

Sonication is a simple method for reducing the size of liposomes. We report the size distributions of liposomes as a function of sonication time using three different techniques. Liposomes, mildly sonicated for just 30 sec, had bimodal distributions when surface-weighted with modes at about 140 and 750 nm. With extended sonication, the size distribution remains bimodal but the average diameter of each population decreases and the smaller population becomes more numerous. Independent measurements of liposome size using Dynamic Light Scattering (DLS), transmission electron microscopy (TEM), and the nystatin/ergosterol fusion assay all gave consistent results. The bimodal distribution (even when number-weighted) differs from the Weibull distribution commonly observed for liposomes sonicated at high powers over long periods of time and suggests that a different mechanism may be involved in mild sonication. The observations are consistent with the following mechanism for decreasing liposome size. During ultrasonic irradiation, cavitation, caused by oscillating microbubbles, produces shear fields. Large liposomes that enter these fields form long tube-like appendages that can pinch-off into smaller liposomes. This proposed mechanism is consistent with colloidal theory and the observed behavior of liposomes in shear fields.

Keywords sonication, liposome, dynamic light scattering (DLS), transmission electron microscopy (TEM), acoustic microstreaming, colloids in shear fields

Introduction

Due to the wide applications of liposomes in biophysics, physiology, and medicine, many techniques have been developed to manufacture them. Among these techniques are reverse-phase evaporation (Parente et al., 1984; Kim et al., 1981), detergent dialysis (Szoka et al., 1980; Woodbury, 1989; Egelhaaf et al., 1996), and simple rehydration. After liposomes are formed by any of these methods they may be reduced in size by extrusion (Hunter et al., 1998; Szoka et al., 1980; MacDonald et al., 1991), high-pressure homogenization (Brandl et al., 1993), or sonication (Huang, 1969). Each technique has merit and

Received 20 June 2005; accepted 17 November 2005.
Address correspondence to Dixon J. Woodbury, Department of Physiology and Developmental Biology, Provo, UT;

can produce small vesicles (<150 nm in diameter) with a fairly narrow size distribution, but none produce a single, narrow population of larger liposomes. Sonication reduces mean diameter, but there is great variability in final liposome size. Sonication could be an effective method of producing liposomes of a desired size if its effects were better characterized. Size is a crucial parameter where liposomes are used as drug delivery vehicles (Lin et al., 2003; Litzinger et al., 1994; Liu et al., 1992), in studies of amphiphysin and other proteins that alter membrane curvature (Peter et al., 2004), and in biophysical studies of channel proteins (Woodbury et al., 1988; Franklin et al., 2004). Not only does a knowledge of liposome size allow calculation of the number of membrane proteins per liposome (given the protein/lipid ratio), it also allows an accurate calculation of liposome content, a parameter useful in drug delivery. Since most methods do not produce a narrow size population of liposomes, it is valuable to know the true distribution of liposome sizes.

Previous studies have shown that liposomes sonicated over a long period of time have a number-weighted distribution that is best fit by the Weibull distribution (Tenchov et al., 1985; Tenchov et al., 1986; Maulucci et al., 2005). The Weibull distribution is a unimodal population similar to the lognormal distribution, but is terminated on the lower-size end at a fixed liposome size. The Weibull distribution is appropriate for liposomes that form from fragments of bilayer sheets and has been used to characterize liposomes after exposure to long, intense sonication. Such liposomes are thought to fragment into small pieces which either reform into liposomes (Maulucci et al., 2005) or undergo secondary particle growth where highly curved small liposomes fuse to form larger liposomes (Lasch et al., 2003).

Using dynamic light scattering (DLS) to measure liposome size, we observe that mildly sonicated liposomes do not fit a Weibull distribution but rather are bimodal. Fig. 1 shows the DLS-determined size distribution for a batch of liposomes prepared by rehydration and sonication for 60 sec in a mild ultrasonic field. The DLS data (deconvoluted by NNLS and CONTIN, see Methods) revealed a bimodal size distribution in most batches of liposomes. This suggests that a different mechanism of liposome formation is occurring with mild sonication.

Little work has been done to characterize the effect of mild sonication on liposome size distribution (Finer E.G. et al., 1972; Zasadzinski, 1986; Egelhaaf et al., 1996; Maulucci et al., 2005). The aim of this paper was to use multiple techniques to measure distributions. To compare results from different techniques, the biases of each technique were taken into account, such as whether measurements are made on individual members of the population or on group averages and on how the data are weighted. Since different assays intrinsically weight data differently, results obtained on the same sample may disagree. To illustrate, Fig. 2A shows a unimodal (thin line) and a bimodal (thick line) distribution that have identical means and standard deviations. For clarity in discussing bimodal populations, the smaller diameter population is termed the alpha population and the larger diameter, beta. It is clear from Fig. 2A that determining just the population mean and standard deviation are not sufficient to differentiate single-peaked (unimodal) from double-peaked (bimodal) distributions. Furthermore, a true bimodal population may be difficult to distinguish from a unimodal one using many common experimental techniques. For example, in DLS, there is always the possibility that the fitting algorithm will merge alpha and beta populations into a single broad distribution. Likewise, a very broad unimodal population may be incorrectly split into a bimodal distribution (Morrison et al., 1985). Other techniques for measuring size distributions have similar weaknesses, such as the loss of peak resolution by making histogram bins too wide when measuring and counting liposomes from an electron micrograph (for an exception see Egelhaaf et al., 1996).

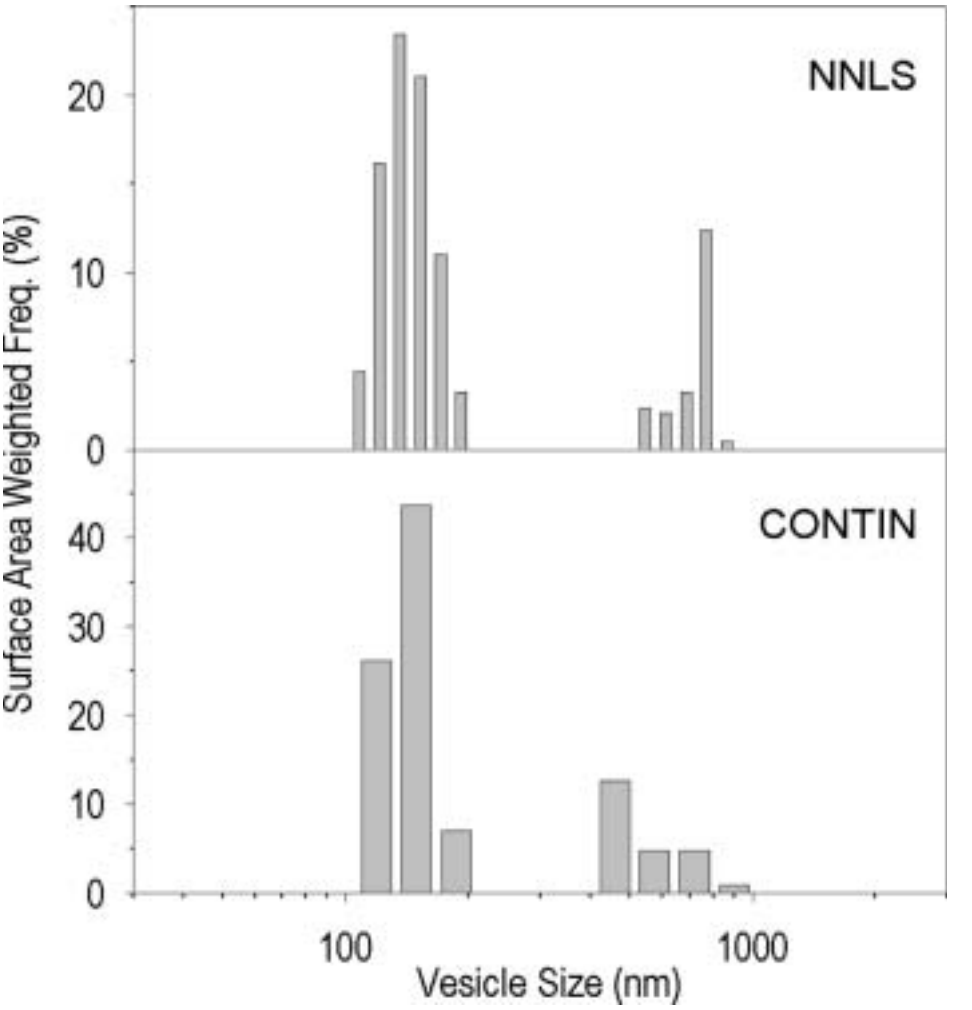

Figure 1. Typical Dynamic Light Scattering (DLS) histograms of sonicated liposomes made as described in Methods. **Top**: The DLS autocorrelation function was deconvoluted using the Non-Negative Least Squares method (NNLS). **Bottom**. The same data as above, deconvoluted using the CONTIN algorithm (see Methods). Notice that both algorithms clearly indicate two peaks representing distinct size populations of liposomes. This sample of liposomes did not contain nystatin and was sonicated for 60 sec.

Statistical weighting of distributions may also be misleading. For example, a bowl of nine grapes and one grapefruit can be described as 90% grapes and 10% grapefruit if the distribution is number weighted, but it can also be described as 10% grapes and 90% grapefruit if the distribution is mass-weighted (Hindes, 1999). A distribution can be weighted by number, surface area, volume, or any other property of the particle being measured. The hypothetical distributions shown in Fig. 2A and 2B represent the same population of liposomes, but are number-weighted and surface area-weighted, respectively. Figure 2A would be observed if the liposomes were counted by taking a picture (e.g., with EM). Figure 2B shows what would be observed if liposomes were first sorted by size (e.g., with column chromatography) and then each size fraction was assayed for

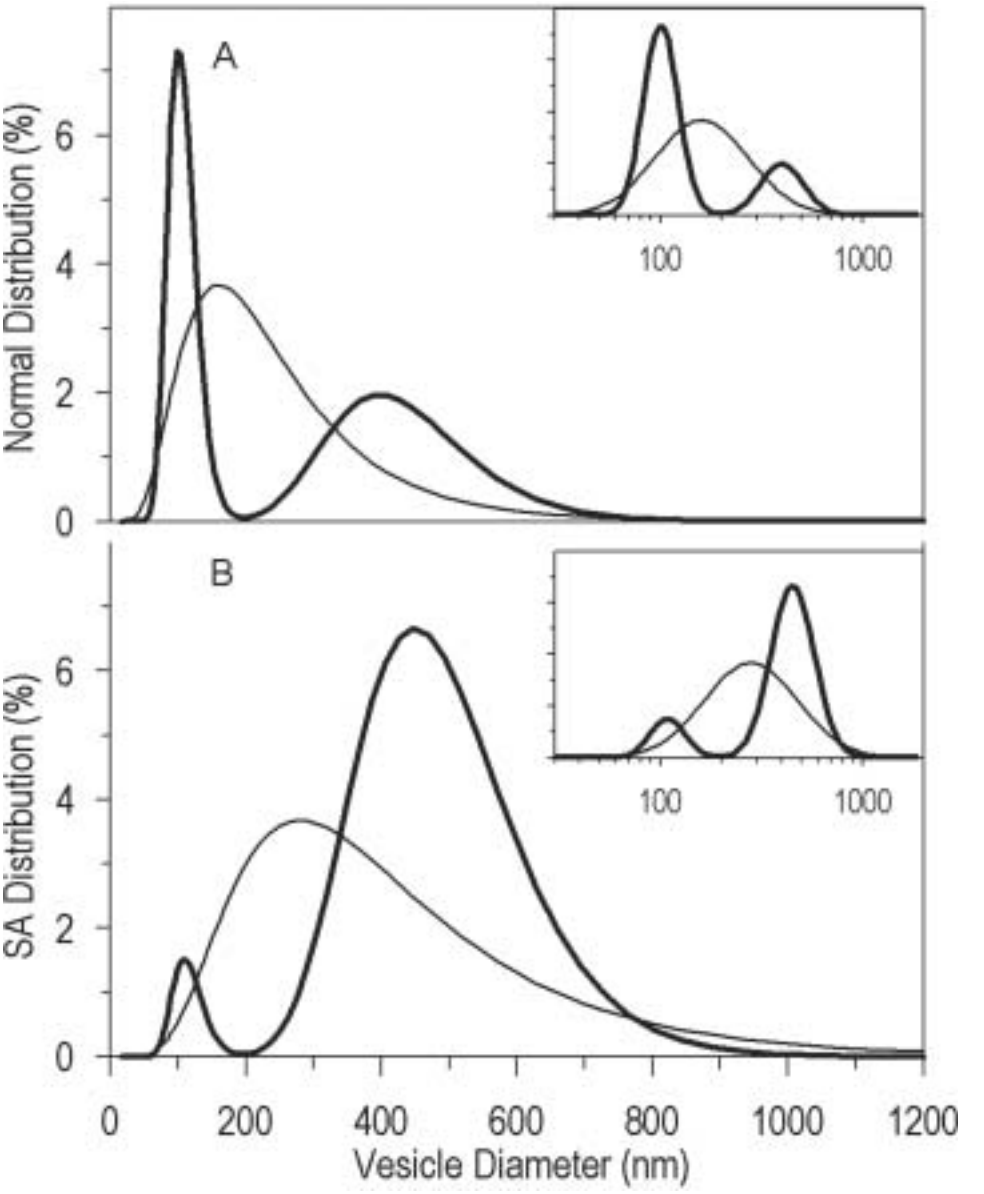

Figure 2. Model comparing liposome populations. **A**. Mathematically generated lognormal distribution of liposomes. The bold line shows a bimodal distribution with means of 100 nm (SD = 20 nm) and 400 nm (SD = 100 nm). The 100 nm diameter liposomes make up 75% (by number) of the total population. Combined, these two distributions have a mean of 180 nm (SD = 102 nm). The thin line represents a hypothetical unimodal liposome population with the same mean and standard deviation as the combined bimodal distributions. **B**. The same bimodal and unimodal populations as in A but surface-area weighted (instead of number weighted). Notice how surface area weighting shifts the distributions to larger liposome diameters. The mean of this SA-weighted bimodal distribution is 408 nm and for the unimodal distribution it is 322 nm. **Inserts**: The same data as in the main figures but plotted on a logarithmic scale.

total lipid. Since the few large liposomes each contribute a large surface area, the surface area-weighted distribution is shifted to the right compared to the number-weighted distribution. Different sizing assays, by their nature, provide different weighting characteristics. Similarly, in different applications results may correlate better with one weighting method than with another. Liposomal delivery of an encapsulated drug, for example, is best described by a volume-weighted histogram to determine the liposome size at which most of the drug is carried. Delivery of a membrane-bound molecule may be better described by a surface-area weighted histogram.

Three methods with different weightings are used to measure the size distribution of mildly sonicated liposomes: DLS, transmission electron microscopy (TEM), and the nystatin-ergosterol fusion assay. The data show that liposomes formed by rehydration/sonication typically form a bimodal size population, and we introduce a simple model that explains this observation.

Methods

Preparation and Sonication of Liposomes

Liposome solutions (0.2 mL) were prepared using a mixture of lipids formed by combining stock solutions (10 mg/mL chloroform) of L-phosphatidylethanolamine (PE), L-phosphatidylcholine (PC), phosphatidylserine (PS), and ergosterol (Erg) in a 2:1:1:0.7 weight ratio (phospholipids from Avanti Polar-Lipids, Inc., Alabaster, AL). Certain mixtures also contained nystatin (Sigma Chemical Co., St. Louis, MO) (2.5 mg/mL methanol) at various concentrations (0–250 μg/mL final sample). Other batches contained only PC as indicated. The mixtures were dried under nitrogen gas. A 0.2 mL solution of 150 mM KCl and 8mM HEPES (pH 7.2–7.4) was added to the dried lipids. The solution was then vortexed 6 minutes and sonicated 90 sec. Liposomes then underwent 1–2 freeze-thaw-sonicate cycles (Pick, 1981) with the last sonication being 30–60 sec or as indicated.

All sonication was performed in a cylindrical, 80 kHz bath sonicator with a diameter of 104 mm (Laboratory Supplies Company, Inc., Hicksville, NY). The sonicator was controlled by a variable transformer set to 75–80 V. The intensity of the sonic waves in the bath is a sensitive function of depth and location. A hydrophone (Type 8103, Bruel & Kjaer) was used to measure the intensity of the ultrasound as a function of position in the bath Sonicator filled with about 450 mL of water. Figure 3 shows that the peak RMS intensity is near the center of the bath (insert). Moving down the central axis of the bath, there are nodes of intensity corresponding to different depths. The surface of the water acts as a node, and the minima and maxima in the bath are presumably due to standing waves of the ultrasound. For liposome sonication, samples were held in the center of the bath at a depth of 5–8 mm. At this depth, liposomes are exposed to approximately 0.7 kW/m^2.

Polystyrene Beads and Carbon Black Preparation

As a control for bimodality, uniform polystyrene beads from Duke Scientific Corporation (Palo Alto, California) of both 102 nm (+/–3) and 404 nm (+/–4) were mixed to a 4:1 volume (mass) ratio in distilled water and prepared for either TEM or DLS analysis. These beads were calibrated to standards from the National Institute of Standards and Technology by the vendor and had hydrodynamic diameters of 100–105 nm and 421–435 nm,

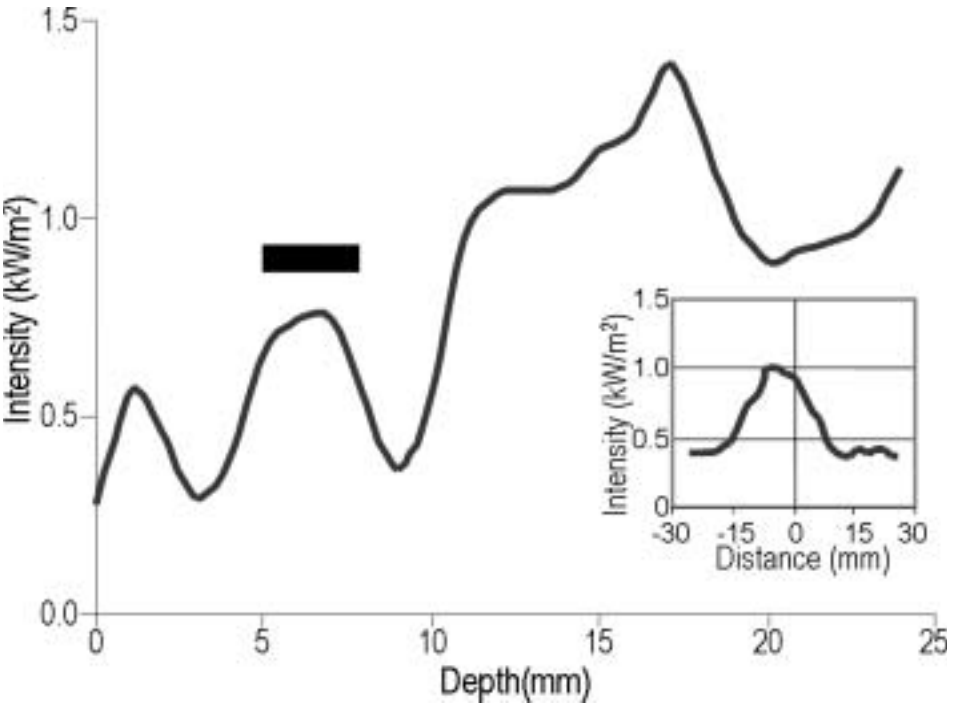

Figure 3. Intensity of ultrasonic energy generated by the bath sonicator as a function of the depth of the sample in the bath. The amount of water in the bath was 430–470 mL and adjusted (tuned) to produce slight splashing at the center of the bath during sonication. The intensity was measured by placing a hydrophone in a 13 × 100 mm glass cuvette (same as used to sonicate liposomes) containing 0.5 mL water. The average of five measurements is shown. The cuvette was moved up and down with a micromanipulator. The thick bar above the graph shows the depth used to in this study to sonicate liposomes (5–8 mm deep). Note that the fluctuations in intensity with depth are about 5 mm apart; this is 1/4 the wavelength of sound in water. **Insert**: A single measurement of intensity as a function of lateral displacement from the center at a depth of 6 mm. Note the peak intensity is near the center.

respectively. As a unimodal control, a sample of Carbon Black was used which had a well-established broad size distribution from 165 nm to 455 nm (Weiner et al., 2002). Carbon black samples were a generous gift of William Bernt (Particle Characterization Laboratories, Novato, California) and were prepared as directed in a 0.1 vol% solution of Triton-X 100 (Columbus Chemical Inc., Columbus, WI) followed by 20 min of bath sonication.

Dynamic Light Scattering (DLS)

All dynamic light scattering (DLS) measurements were performed using a *Brookhaven 90Plus* Particle Size Analyzer (Brookhaven Instruments Co., Holtsville, New York). The incident angle of the laser was 90° with a wavelength of 658 nm. Samples were diluted in their original buffer in 4 mL cuvettes to count rates of 200–1000 kcps. Sample temperature was maintained at 22°C. The parameters used for the deconvolution algorithms with DLS included 0.96 cP for viscosity. For all aqueous solutions the refractive index was 1.33 and for particles, the real refractive index was 1.53 (liposomes), 1.59 (beads), or 1.84

(carbon black). The particle imaginary refractive index was set to 0 (beads and liposomes) or 0.85 (carbon black). For liposomes, hundreds of samples were initially prepared and analyzed by DLS to determine effective diameter. Follow up studies on over 80 liposome samples were prepared, and 5–10 parallels of 2.5 min each obtained (over 500 runs). For carbon black and bead samples, 16 parallel runs of 10–30 min each were obtained. Fresh dilutions of the original samples were prepared and the parallel runs repeated. Nearly identical results were obtained both times.

The DLS autocorrelation function of scattered light was deconvoluted using the Method of Cumulants, the Non-Negative Least Squares (NNLS) method, and a Constrained Regularization Method for Inverting Data (CONTIN) as implemented on the 90Plus Particle Size Analyzer. The Method of Cumulants assumes a unimodal population and returns an average, or "effective" diameter of the distribution, and a unitless measure of the width of the distribution (polydispersity) (Koppel, 1972). The NNLS algorithm uses fewer assumptions and can identify bimodality well, but may incorrectly separate a single broad population into multiple narrow populations (Morrison et al., 1985). CONTIN is based on NNLS, but has a smoothing feature to compensate for false bimodality (Provencher, 1982; Morrison et al., 1985). Morrison reports that "Our experience with CONTIN has been that the smoothing of the distribution works well when smooth distributions are expected. However, the method works less well when multimodal distributions are expected." That is, CONTIN may overcompensate and smooth two peaks into one. Since we did not initially know what type of distribution to expect, DLS data were initially analyzed by both procedures (e.g., Fig. 1). Unless otherwise stated, all DLS population distributions shown in the figures were deconvoluted by NNLS. This study focuses on liposome 20–2000 nm in diameter. Particles outside this range made little contribution (typically <1%) to the total liposome population and were irregularly observed. Particles smaller than 20 nm in liposome samples were also ignored because curvature considerations prevent liposomes (with our lipid composition) in this size range (Israelachvili, 1985; Rovira-Bru et al., 2002; Lasch et al., 2003; Epstein et al., 2005).

Transmission Electron Microscopy (TEM)

Polystyrene beads, Carbon Black, and liposome samples were prepared by negative-staining in Urinyl Acetate as previously described (Woodbury, 1989). While other techniques such as cryoelectron microscopy have certain advantages, negative-staining is a fast, easy technique that does little to alter relative liposome size. Samples were analyzed at various magnifications using a JEM-2000FX electron microscope (JEOL USA Inc., Peabody, MA). Resulting photographs of beads and liposomes were measured by hand. Carbon black and beads were assumed to maintain their three-dimensional structure. Liposome diameters, however, were corrected by a factor of 0.707 due to flattening by dehydration (Parente et al., 1984; Szoka et al., 1980). There is some controversy over the use of this factor (Drechsler et al., 1995). In fact, our data (see Table 2) suggest that a factor of 0.89 is more correct. Nevertheless, to be consistent with previously published data we have retained the 0.707 factor (which does not alter the ratios given in the final column of Table 2). Carbon Black, due to its irregular shape, was measured using AlphaEaseFC software (Alpha Innotech Co., San Leandro, CA). The program distinguishes the borders of carbon black aggregates and returns a cross-sectional surface area for each particle region. This surface area was transformed into an equivalent spherical particle size (diameter) as $d = 2\sqrt{SA/\pi}$.

For liposomes, size distribution histograms of the same TEM field at three different magnifications yielded significantly different population modes. Further analysis revealed that due to the transparent nature of liposomes, many smaller liposomes are only visible at higher magnifications, while many large liposomes extend out of field and are easily missed (e.g., compare Fig. 9A and 9B). Therefore, caution must be exercised when analyzing liposome size distributions at only one "optimal" magnification. The histogram (Fig. 9C) was created from the combined data of the three magnifications (×1,700, ×5,000, and ×17,000). The histograms were spliced together in such a way that the higher magnification data were used for small sizes until a bin size was reached that had the same number of liposomes as that obtained at lower magnifications. The absolute number of liposomes in this bin was used to scale the two data sets (the high magnification EMs always scored more liposomes in the same field then lower magnifications).

Nystatin-Ergosterol (Nys/Erg) Fusion Assay

The nys/erg fusion assay (Woodbury, 1999; Woodbury et al., 1990) was used to detect the fusion of single liposomes to a lipid bilayer. At appropriate concentrations, nystatin and ergosterol form ion channels in liposomes. When liposomes fuse to a planar membrane, a sharp increase in membrane conductance can be detected with each fusing liposome. The spike decays quickly as the liposome's nystatin channels become unstable in the ergosterol-free membrane. The current signal is proportional to the number of nystatin channels in the liposomes' membrane. The channels are assumed to be evenly distributed throughout all liposomes. Since each liposome fusion event is detected by the assay, the raw data is number weighted; however the diameter of the fusing liposome is proportional to the square root of the current spike height. Conductance measurements were acquired with a standard data acquisition system (Woodbury, 1999), and the spike height of each fusion event was measured by hand. Higher [nys] were used in some experiments to help resolve alpha liposomes (the nys channel is too small to detect a single channel, so alpha liposomes with only a few channels can not be detected). Likewise, beta liposomes with many nystatin channels produce a current that saturates the voltage-clamp amplifier and again cannot be measured. Liposomes with many channels may also be too leaky to fuse (Woodbury et al., 1988). Therefore, some experiments were performed with a lower nystatin concentration to ensure that large liposomes could be detected. Each fusion experiment was run for 10 min (Woodbury, 1999).

Statistical Methods

To compare size distribution histograms from different techniques the data must be weighted similarly. Transformations between weightings are easily done assuming spherical particles. Surface area weighting is then proportional to the square of the number weighted data; volume is proportional to the cube, and so forth.

All histograms, unless otherwise specified, are presented as surface area-weighted distributions with logarithmic size bins (normalized with width of bin). Surface area-weighted histograms are presented because when sizing liposomes, total lipid is proportional to liposome surface area. DLS is inherently an intensity-weighted technique, that is, the primary measurement is the intensity of light scattered from liposomes diffusing through the laser light path. However, this raw data can be transformed (with built-in software) to give a surface-area weighted histogram. The nys/erg fusion assay

is a number-weighted technique that reports liposome surface area (i.e., each fusion is detected or counted independently, but the size of the signal is proportional to liposome surface area). EM is number weighted (liposomes or particles are counted independently) and liposome diameter is determined directly or estimated from the cross-sectional area. A second advantage of using surface area-weighted data is because it is intermediary between number- and volume-weighted data. When a population distribution is transformed over several spatial dimensions, the shift in weighting can cause one size to appear to dominate the population, or it may misleadingly disappear (see Fig. 2).

All "peak" values referred to in the results are the mode of the distribution unless otherwise specified. Modes were chosen over means due to their insensitivity to outliers and ease of detection. However, it is clear from the figures that in most cases, the mode approximates the mean.

Results

In our initial studies we were interested in general trends in population size as a function of both sonication and the antifungal agent nystatin. We prepared hundreds of samples and used DLS Method of Cumulants to determine effective (mean) diameter and polydispersity (a measure of standard deviation). Although further analysis later determined that most of these samples had bimodal population distributions (see below), the effective diameter (which gives a weighted mean based on all vesicles) still provides a simple and reliable measure of average vesicle size and how it changes in response to sonication. Figure 4 shows the effective diameter from over 500 samples of liposomes prepared in our lab, determined by DLS. As expected, with increased sonication time, there is a decrease in both effective liposome diameter and polydispersity. Liposomes were prepared with various concentrations of nystatin. This antifungal agent did not alter the effects of sonication on liposome size (Fig. 4).

As noted above, further liposome analysis by DLS revealed that the size distribution is bimodal, not unimodal, and that the effective diameters shown in Fig. 4 are an oversimplification of the effect of sonication on liposome size. Figure 2 shows that effective diameter and polydispersity are inadequate to properly describe a bimodal population. Together these data suggest that the decrease in mean diameter observed in Fig. 4 could be due to a true decrease in the size of most liposomes, or a shift of a few liposomes from a beta (larger) population to an alpha population. A third possibility is a combination of both processes.

To better understand the true size distribution of the liposome populations, the DLS autocorrelation function was deconvoluted using NNLS and CONTIN (see Fig. 1 and Methods). We expected a single, broad lognormal or Weibull distribution, but consistently observed two distinct peaks within the appropriate size range. A typical example is shown in Fig. 5 and shows that the decrease in mean size (Fig. 4) is due to both a decrease in the size of most liposomes and the shifting of liposomes from the beta population to the alpha population. Typically with sonication, the peak representing the beta population of liposomes is more variable and decreases in diameter and percentage of the total population. The alpha population of liposomes decreases slowly in size and grows in percentage to dominate the total population. Both peaks seem to approach a lower size limit of around 50 and 150 nm, respectively. Bimodal populations in liposomes are observed even after 1h of sonication. Note that the ratio of the peaks is greater

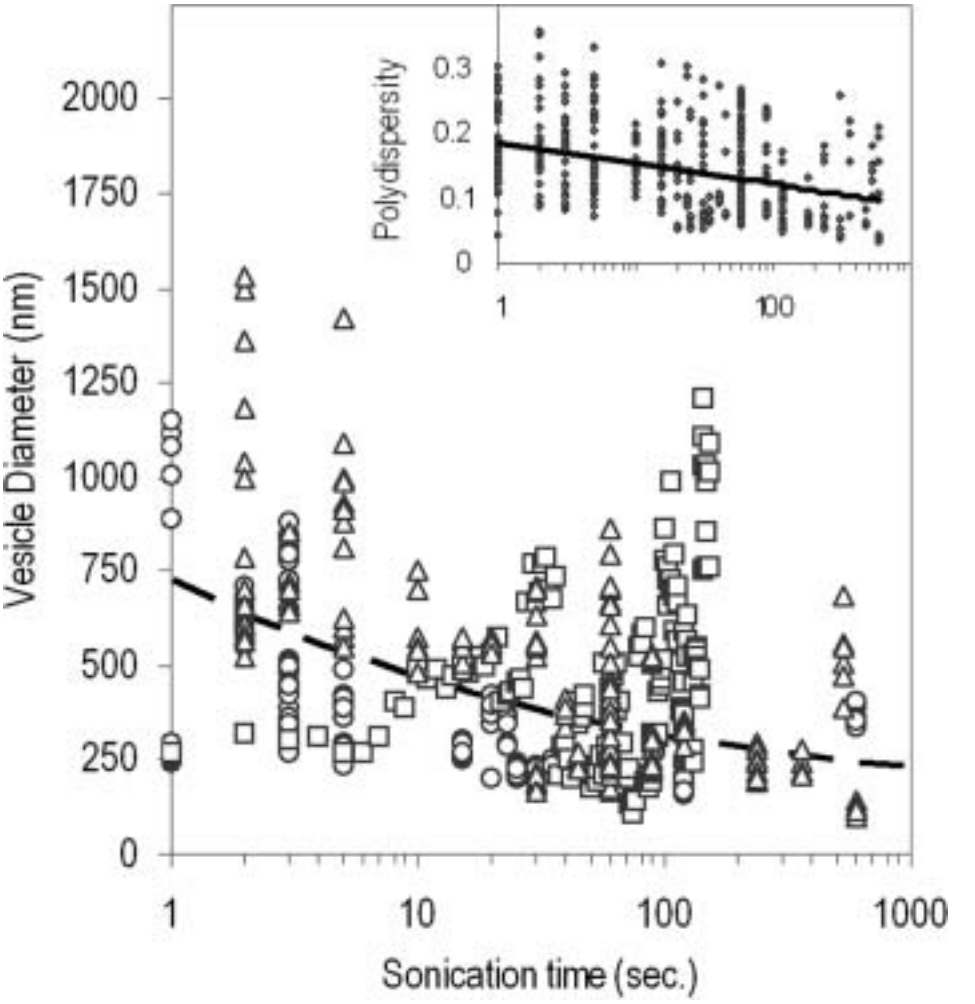

Figure 4. Effect of sonication time on mean diameter and polydispersity of liposomes as measured by DLS. The mean is determined from the whole population of vesicles and does not imply a unimodal distribution. For each sample, 4 to 7 DLS runs (~2.5 min each) were performed on liposomes exposed to various durations of sonication. The average of these runs is plotted. Over 500 samples were analyzed. **Insert**: Polydispersity (unitless measure of distribution breadth) of the same data set. Note the downward trend in both plots. There was no significant correlation between liposome size and nystatin concentration: ❍ = 28–56 μg/mL Nys, Δ = 75–85 μg/mL, □ = 113–153 μg/mL.

than two, which is the lower limit of DLS peak resolution (Korgel et al., 1998; Finsy et al., 1993).

To compare the DLS data from all 82 liposome samples, a modification of the procedure purposed by Frantzen et al. (2003) was used. DLS parallel runs (5–10) of 2.5 min were made on each sample and the NNLS-determined distribution that appeared most frequently was recorded. As reported in Table 1, over 85% of liposome samples were bimodal (with the remainder split equality between unimodal and trimodal). Several of the samples listed as unimodal were bimodal, but with a small second population in

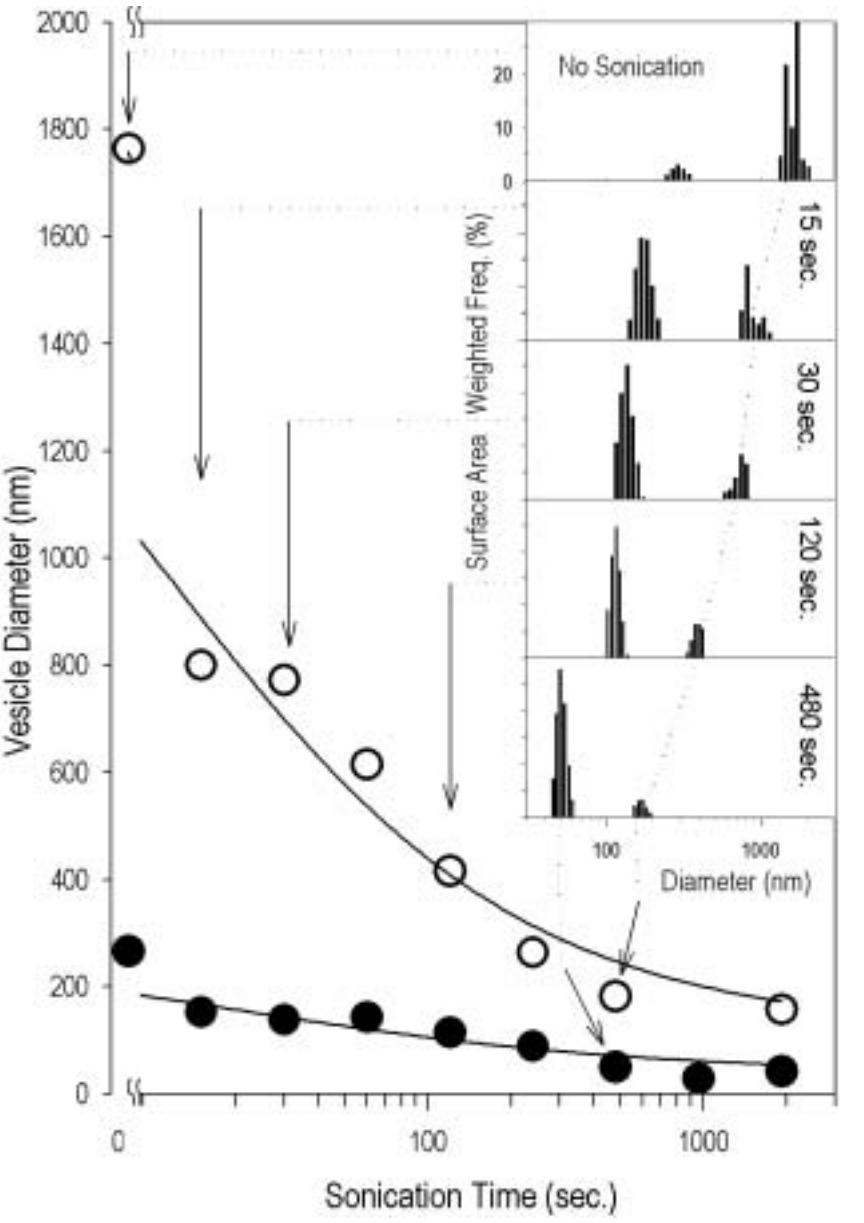

Figure 5. One typical experiment showing the decreasing trend of liposome size with duration of sonication. Note that there are two populations detected (except at t = 960 sec). The mode of the alpha (larger-size) population is shown on the main graph with open circles and the beta (smaller-size) population with closed circles. Consistent with Fig. 4, increasing sonication time (x-axis) causes a gradual decrease in liposome size. **Inserts**: Selected individual DLS histograms (analyzed by NNLS and weighted by surface area) at indicated sonication times. The inserts clearly show that with no sonication the population of large liposomes accounts for a majority of the total population. Following sonication, the smaller-sized liposomes become the dominate population. (As described in methods, the "no sonication" liposomes were actually sonicated for 90 sec and then frozen; without this treatment, an even larger fraction of liposomes have diameters >1000 nm.)

Table 1
Modality of liposome populations determined using DLS (NNLS). Table combines data from 82 sample and includes 500 parallel runs

	# Liposome samples with distribution shown			
	Unimodal	Bimodal	Trimodal	Total
Results from all parallels (5–10 per sample)	6	70	6	82
Results excluding parallels with residuals>10 and samples with <4 parallels	3	68	6	77

the range excluded (>2000 nm). An additional criteria recommended by Frantzen et al., is to exclude parallels with residuals >10. With this constraint, 8.6% of the 500 runs are excluded. This constraint only slightly altered the results (Table 1) and was not used.

Beads and Carbon Black

One concern with using DLS to determine the size distribution of particles is that the deconvolution algorithms may misinterpret the data. To independently confirm that DLS can correctly detect two known and distinct populations close in diameter (Korgel et al., 1998), a mixture (4:1 mass ratio) of 100 and 400 nm polystyrene beads was prepared and analyzed. Figure 6 shows that the NNLS deconvolution algorithm clearly resolves two distinct peaks. According to DLS, the alpha peak had a mode of 92 nm (SD = 10 nm). The beta peak had a mode of 431 nm (SD = 41 nm). These values agree well with the hydrodynamic diameters (100–105 nm and 421–435 nm) reported by the vendor for these beads and are consistent with more extensive studies done with mixtures of smaller beads (Frantzen et al., 2003).

It also was a concern that the observed bimodal distribution of liposome sizes could be a misrepresentation of a very broad but unimodal population divided by the deconvolution algorithm into two populations. To determine if DLS can properly detect unimodal distributions with a broad standard deviation, a specific carbon black sample was analyzed with a previously reported unimodal size distribution spanning the same size range as the beads. DLS data were acquired (duplicate sets of 16 parallels of 10–30 min) from the carbon black sample. Deconvolution by CONTIN and NNLS reported a broad unimodal population with particles ranging from 75 to 500 nm in diameter. With CONTIN all parallel runs were unimodal; NNLS also gave a unimodal distribution (recorded in 70 percent of the parallels). Fig. 7A is an example from one DLS run using NNLS analysis.

Transmission Electron Microscopy (TEM)

TEM is another way of validating the population distributions observed using DLS. TEMs of carbon black (Fig. 8A and 8B) show many irregular particles. The effective size of the particles was computed automatically as described in methods. Fig. 7B shows the size distribution of the particles in Fig. 8. This distribution, determined by

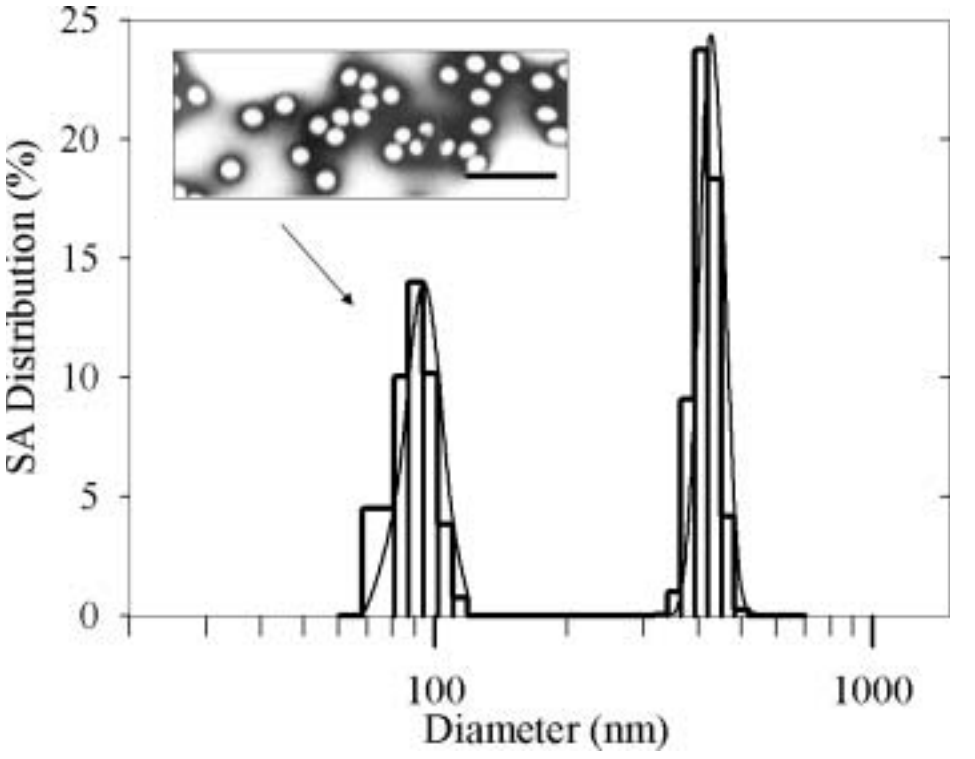

Figure 6. Bead calibration of DLS. A 4:1 mixture of 102 nm and 404 nm polystyrene beads was diluted and sized using DLS. One typical measurement is shown (4 h sample time). DLS consistently distinguished two separate populations that were only 300 nm apart. **Insert**: Electron micrograph of 102 nm polystyrene beads taken at ×34,000. The length of the bar is 500 nm.

TEM, is a little broader than that determined by DLS (Fig. 7A), although the means are similar and match the previously reported distribution (Weiner et al., 2002). The hint of a beta population in Fig. 7B could be a counting artifact. The irregular shape of carbon black particles made it possible to mistake two overlapping particles as one larger particle thus producing a spurious beta population in the size distribution histogram. This indication of bimodality in the TEM-determined distribution is not observed in the DLS-determined distribution. Taken together, these data show that the NNLS deconvolution algorithm is not biased toward producing a bimodal distribution from a broad unimodal distribution.

Liposomes with 30 seconds of sonication were also analyzed by TEM (Fig. 9). The histogram (Fig. 9C) was created from the combined data of three different magnifications (see Methods) and indicates a bimodal population with modes of 110 and 600 nm. These values support those obtained by DLS at 30 sec sonication (Fig. 5) of 140 and 750 nm.

Nys/Erg Assay

The nys/erg assay provides a third method to determine the size distribution of the liposome population, although only relative sizes can be measured. The assay was performed on >100 liposome samples with several different concentrations of nystatin. The assay detects the fusion of liposomes with a planar lipid bilayer. Each fusion event is

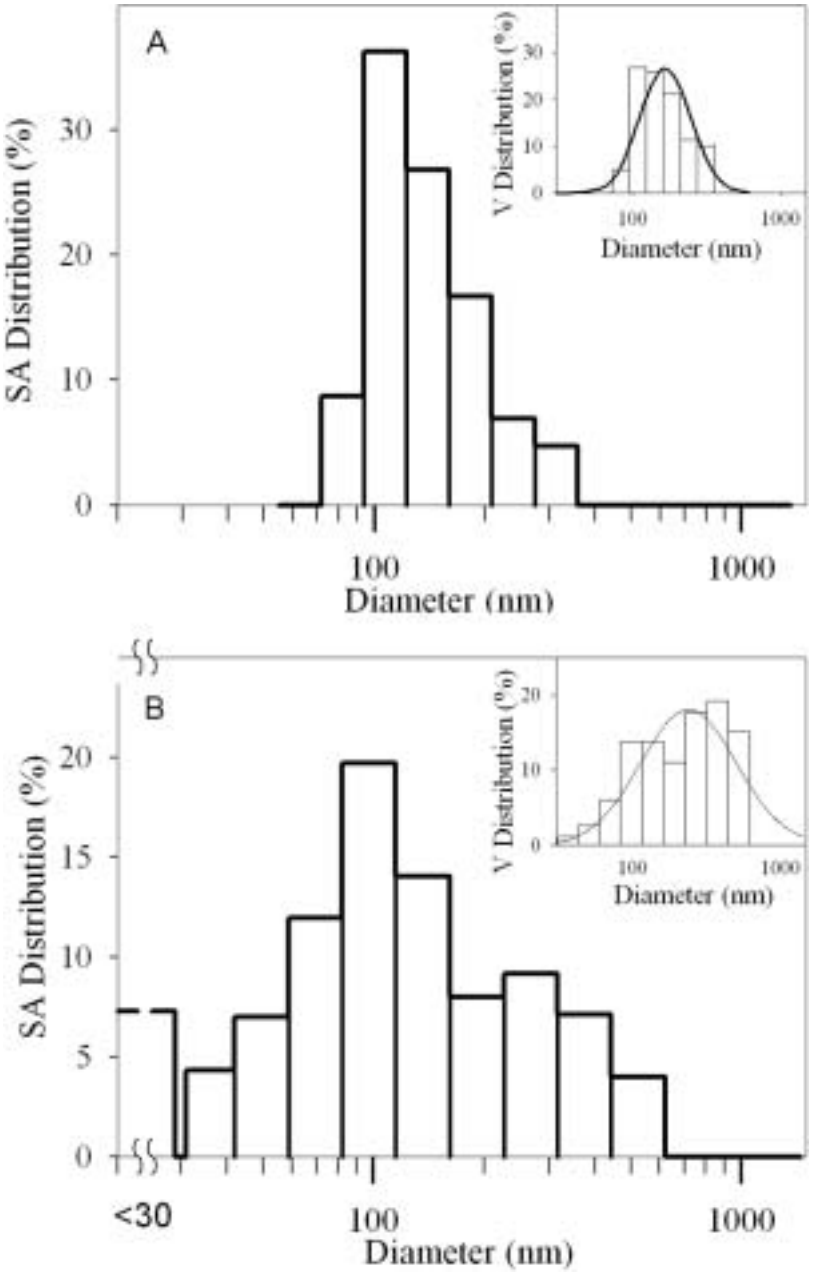

Figure 7. A. Carbon black calibration of DLS. A typical DLS run of carbon black is shown. According to DLS (NNLS deconvolution shown), carbon black particle sizes form a unimodal distribution and range from 75 nm to 350 nm with a mode of 123 nm (surface area weighted). This is in agreement with results on this type of carbon black previously published (Weiner et al., 2002). **B.** Histogram of carbon black particle size by TEM. The particles in Fig. 8A were analyzed as described in Methods. Note the broad distribution of sizes from <30 nm to 600nm. The absence of a second population in DLS measurements (A) gives credence to the bimodality observed in liposomes. **Inserts**: Same data but weighted by volume, as reported by Weiner (Weiner et al., 2002).

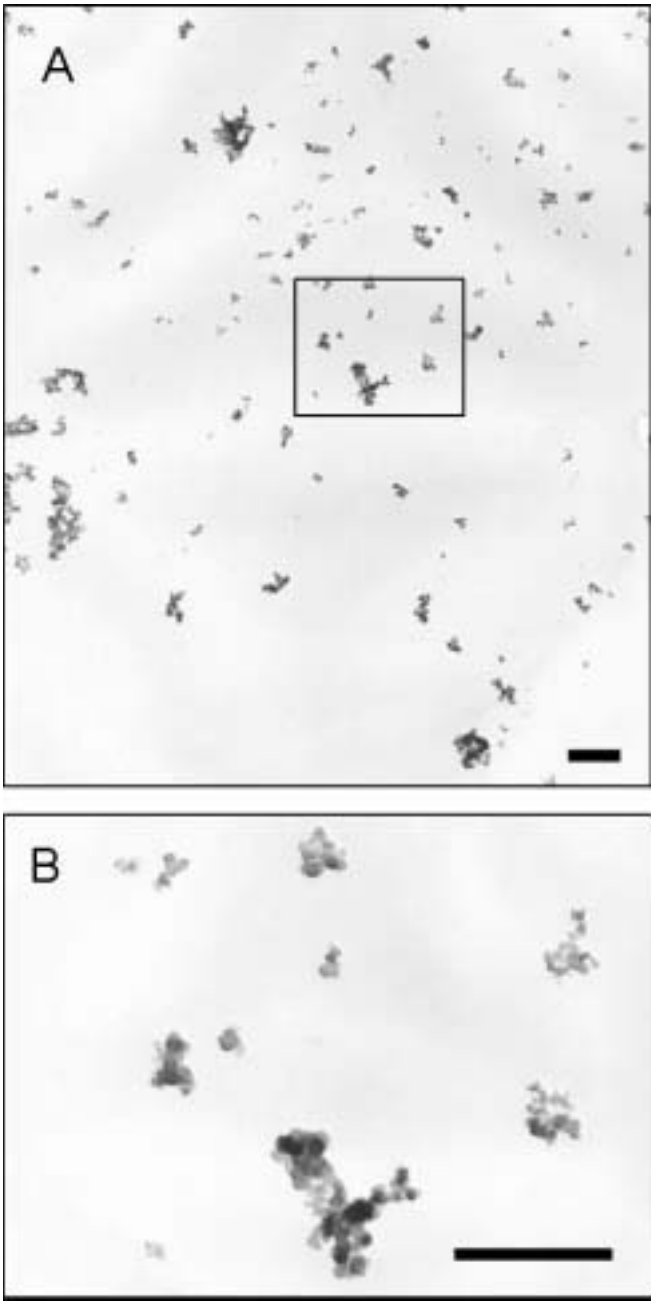

Figure 8. Electron micrographs of carbon black. **A.** Typical carbon black micrograph taken at ×10,000. **B.** Enlarged view of area outlined in A. Although large particles appear to be aggregates of smaller globules, they must be fused together since treatment by detergent, sonication, and dilution did not separate them. In each micrograph, the length of the bar is 500 nm.

marked by a sudden spike in bilayer conductance proportional to the number of nystatin channels in the liposome membrane. Thus, the conductance increase is a measure of

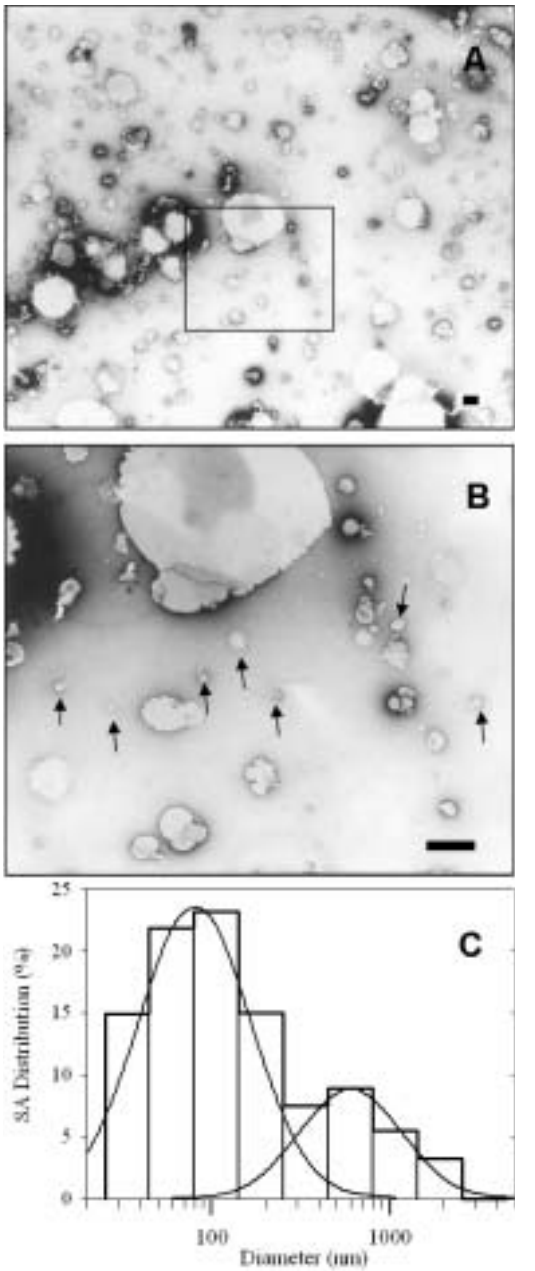

Figure 9. Electron micrograph of liposomes. Liposomes (56 μg/mL nystatin) were sonicated for 30 sec and then analyzed with TEM. **A** shows a typical micrograph taken at ×5000. **B** shows the field outlined in part A at ×17,000. Arrows highlight some of the liposomes with diameters of about 100 nm which are not visible in A. In each micrograph, the length of the bar is 500 nm. **C**. TEM histogram of liposomes. Multiple corresponding visual fields were counted by hand three times (by different observers) from micrographs taken at ×1700, ×5000, and ×17,000. All data from micrographs (~320 liposomes counted three times) were combined to produce this histogram. The lines show two lognormal distributions that fit the data. Note that the means of these two distributions (110 and 600 nm) agree well with the DLS data in Fig. 5 at 30 sec.

liposome surface area. Most experiments contained 50–150 spikes. The spike heights from all experiments were combined into the normalized distribution shown in Fig. 10. Different data symbols are used for the different nystatin concentrations since higher [Nys] will give larger signals for the same size liposome. To align the data with different [Nys] we assumed that the Nystatin conductance has a sixth-order dependence on concentration (nystatin channels form by aggregation of six or more nystatin monomers) (Moreno-Bello et al., 1988). The fit was not greatly altered if a higher-order dependence was assumed. The distribution is number-weighted (since each liposome fusion is detected independently) but the binning is by surface area (proportional to spike height).

The data are well fit with a bimodal distribution (see figure legend for parameters of fit). Note that the lower [Nys] concentration was optimal for observing the alpha population of liposomes and the higher [Nys] was best for observing the beta liposome population.

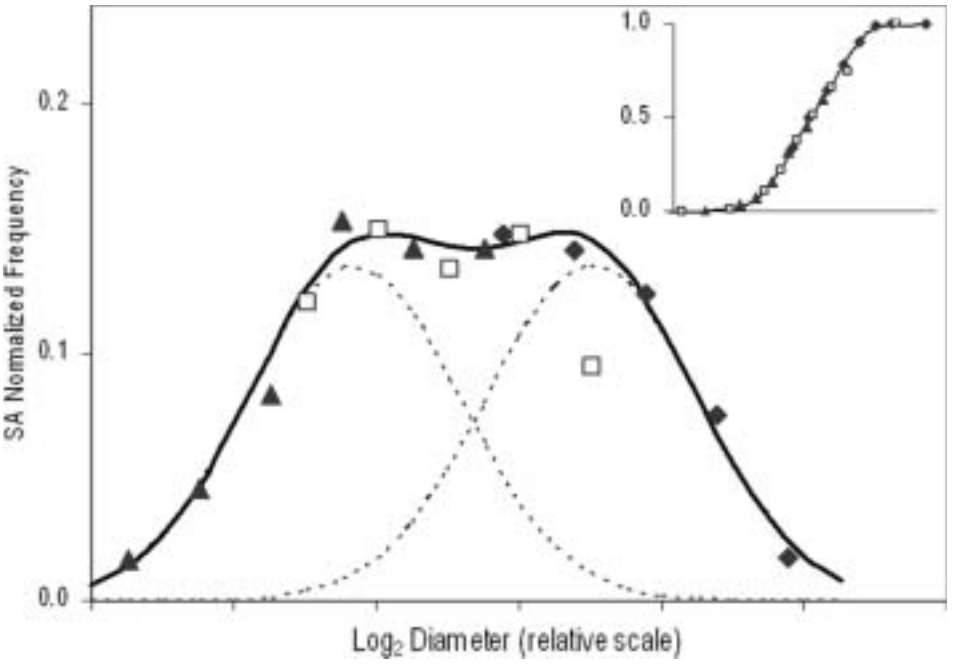

Figure 10. Frequency distribution of fusing liposomes based on nystatin conductance. Using the Nys/Erg Fusion Assay, liposomes with a low (♦ = 28 and 56 μg/mL), medium (□ = 85 and 113 μg/mL), and high (▲ = 250 μg/mL) concentrations of nystatin, were fused to a planar bilayer. The spike in bilayer conductance when a liposome fuses was recorded and binned for each concentration. The frequency was then normalized to produce this figure. The x-axis is the square root of conductance and is proportional liposome diameter. The three data sets, have been shifted along this axis based on the assumption that conductance is a sixth-order function of [Nys] (see methods). **Insert** shows the cumulative distribution for all three data sets overlaid (x axis is same as main figure). The best cumulative fit was found with the following parameters: Equilibrium constant for formation of Nystatin hexamer channel Ke = 0.03; for high [Nys] the percent of liposomes too large to observe = 40%, for low [Nys] the percent of liposomes too small to observe = 35%, and for med [Nys] the percent of liposomes too large to observe = 25% and too small to observe < 2%.

Although the data are somewhat crude and do not give absolute sizes, the observed distribution is consistent with the bimodal distributions observed with DLS and TEM.

Discussion

Liposomes are usually described by their mean size; however, we show that mildly sonicated liposomes generally have a bimodal size distribution and are not well described by a single mean. The bimodality of sonicated liposomes is confirmed using multiple independent techniques. Although the bimodality was most apparent using DLS (Table 1 and Fig. 1 and 5), both TEM (Fig. 9) and the nys/erg fusion assay (Fig. 10) gave supportive results. Table 2 summarizes our data for 30 sec of sonication.

We were concerned that the DLS data could be biased in the deconvolution algorithm and that the true population distribution was simply very broad but unimodal. To test this possibility a sample of carbon black (soot) with a known broad unimodal size distribution was analyzed by both TEM and DLS. TEM analysis (Fig. 7B) supported a unimodal distribution for the carbon black, but also contained a small shoulder that could indicate a second (beta) population. Nevertheless, DLS analysis (Fig. 7A) consistently gave a broad unimodal distribution, strongly supporting the conclusion that the bimodal distribution of liposomes observed with DLS is not an artifact of the deconvolution algorithms.

This conclusive evidence of a bimodal population of liposomes led us to explore the mechanism whereby mild sonication reduces liposome size. Current theories postulate that sonication, as with other methods of liposome formation, randomly fragment multilamellar vesicles (MLV) into what are termed bilayer phospholipid fragments (BPF) (Korgel et al., 1998; Lasic, 1987; Lasic, 1988). These disc-like fragments are thought to fold up into thermodynamically stable liposomes (Fromherz, 1986; Fromherz et al., 1985). Alternatively, tiny unstable liposomes, formed during sonication, may fuse together to form slightly larger, stable liposomes (Lasch et al., 2003; Brandl et al., 1993). The result of such random, uniform fragmentation can be fit using the Weibull distribution, which describes the size distribution of particles undergoing such a process. Other theories have also been presented (Zasadzinski, 1986; Finer E.G. et al., 1972), but the BPF mechanism seems to describe best the phenomena of liposome formation by high-energy sonication (Lasic, 1988).

The populations dynamics observed in this study cannot be described by such a mechanism. We observe two separate size populations. The beta population starts out as a broad population with a large diameter while the alpha population is smaller and narrower. As shown in Fig. 5, sonication appears to create alpha liposomes from the larger beta ones, perhaps by causing alpha-sized liposomes to pinch or bud off from beta liposomes. In

Table 2

Three techniques were used to determine liposome size (DLS, TEM, and the Nys/Erg assay). Due to the nature of the Nys/Erg assay, the absolute size of the alpha and beta populations cannot be determined; however, their existence is observed and the ratio between them can be calculated

	Liposome size following 30 sec of sonication		
Sizing method	α-Population	β-Population	Ratio β/α
DLS	140 nm	750 nm	5.36
TEM	110 nm	600 nm	5.45
NYS/ERG	–	–	3.2

addition, the mean size and width of both alpha and beta populations slowly decrease and the effective mean diameter of the alpha approach 40–50 nm after an hour of sonication. This reduction in size of the alpha population may be due to BPF.

In one of the first papers on the sonication of liposomes, Huang hints at similar population dynamics (Huang, 1969). Using chromatography, he found that sonicated PC liposomes can be separated in two fractions: a large beta population that eluted with the void volume, and a small, homogeneous alpha population of about 25 nm. Huang also observed the relative amounts of the fractions depended on the time of ultrasonic irradiation. The alpha population became the major fraction after longer periods. He states that under no conditions was the beta population completely absent after sonication. Finer (Finer E.G. et al., 1972) and others found similar trends. Nevertheless, Huang and most workers in the field have discounted this larger population as a remnant or artifact and its existence is largely ignored.

The bimodality shown by this study and by others suggests that a mechanism other than uniform fragmentation is involved when liposomes are exposed to mild sonication. Before proposing a new mechanism it is useful to review the known effects of sonication. During sonication, a rapidly oscillating transducer produces ultrasonic (>20 kHz) waves that travel through water. These pressure waves interact with microbubbles of air. The high-pressure cycle compresses the bubbles to a fraction of their original size. The bubble expands in the low-pressure cycle of the wave, and the bubble continues to oscillate with each passing wave. This oscillation of microbubbles is known as cavitation. If the ultrasonic intensity is high, or if the bubble size is near resonance for the applied frequency, the bubble can be compressed adiabatically to a very small volume, causing local temperatures and pressures up to 10,000 K and 1,000 bar (Nyborg, 2001; Sundaram et al., 2003). Such violent compression is called “collapse” or “inertial” cavitation.

One possible mechanism for the formation of alpha liposomes comes from a consideration of cavitation forces. It has been established that dense particles in a sound field are attracted to the source of sound. During cavitation, oscillating microbubbles set up their own local sound field and exert an attractive force, called radiation force, on nearby particles. Theoretical calculations show that a typical oscillating bubble in a 2 MHz sound field can induce accelerations of 300,000g on local particles (Nyborg, 1982).

We propose that this radiation force is responsible for the first step in alpha liposome formation by sonication. Since the liposomes used in these studies can be pelleted in an ultra centrifuge, the lipid shell is denser than the surrounding water. A bubble 80 μm in diameter (the resonant size for 80 kHz ultrasound, see Eq. 4 in Nyborg, 2001), could easily have an attractive force on beta liposomes. These liposomes would be quickly drawn closer to the large cavitating bubble by the radiation force.

The second step we propose in alpha liposome formation occurs near the surface of the oscillating bubble. The flow of liquid around a sphere expanding and contracting at ultrasonic frequencies is quite complex. This flow has been characterized using simple models such as oscillating cylinders (Nyborg, 1968), wires (Williams et al., 1970), and visual observations of hemispherical bubbles (Elder, 1959). As shown in Fig. 11, a symmetrical pattern of circular eddies is setup near the surface of the bubble. These patterns of flow, referred to as acoustic microstreaming, produce very large velocity gradients. The resultant shear fields deform and shear liposomes (Marmottant et al., 2003). It has been shown that hemolysis can be induced by the shear forces from microstreaming without other effects of sonication (Williams et al., 1970). Nyborg (Nyborg, 1968) showed dependency of the shear field on frequency, amplitude and other parameters of the ultrasound. We propose that these shear fields are responsible for the formation of alpha liposomes from beta liposomes.

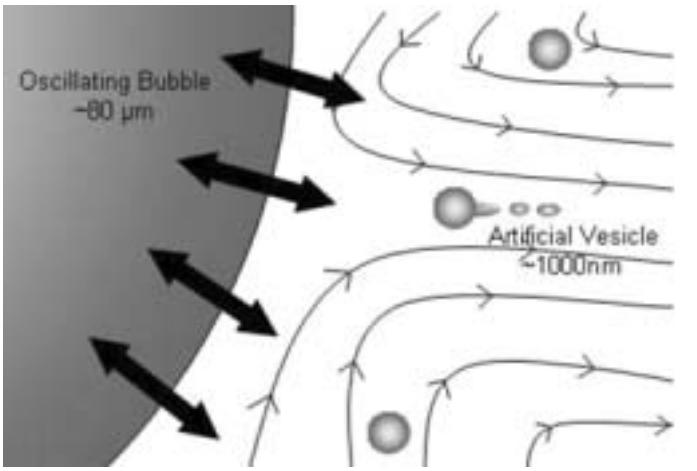

Figure 11. Illustration of a liposome entering the shear field of a cavitating bubble. The large bubble (left) is oscillating (bolded arrows). Smaller, curved lines with arrows represent the variable flow of fluid caused by such oscillation (acoustic microstreaming). Microstreaming is postulated to drive tube formation (right).

Recent research in fluid dynamics provides some details of how liposomes are altered by shear fields (Kraus et al., 1996; Mendes et al., 1997; Shahidzadeh et al., 1998; Abkarian et al., 2002). Shahidzadeh (1998) observed that in shear fields, small tube-like structures extend from the liposome surface. Colloidal theory and basic physical chemistry describe what happens to such structures as they lengthen. An immiscible fluid column inside another fluid may be stable depending on the velocity of the stream and the length of the column. However, when the inertial forces are overcome by surface tension, a tube-like structure will separate into small, somewhat uniform spheres. As shown in Fig. 11, we propose that protrusions from a liposome, produced by shear, become longer until inertial forces are overcome by the lipid's own surface tension. As they become unstable, they pinch off into smaller alpha liposomes. Hence the large beta population is diminished in both size and number as the uniform alpha population emerges to dominate the distribution. This mechanism is consistent with the population dynamics shown in Fig. 5. In such a process, some lipid tubes may be stable and remain long after the sonication process, providing evidence of the previous exposure to shear fields.

In 1989, we reported an observation with TEM of stable long, tube-like lipid structures following sonication of liposomes (Woodbury, 1989). Upon using TEM to count liposomes for the size distributions reported here, similar structures were again observed (Fig. 12A). Additionally, some images showed long undulating tube-like structures with smaller liposomes apparently pinching off of one end (Fig. 12B and 12C). Note that in Fig. 12B the tube undulations and nearby liposomes are 50–100 nm, consistent with the size of the alpha population of liposomes. These tubular structures may be artifacts of lipid layers hydrating on the surface of a MLV as reported previously (Lasic, 1988). Another possibility is that these tubes and undulations are artifacts of the TEM staining/drying process. However, we have also observed stable lipid tubes in aqueous liposome samples using enhanced light microscopy (data not shown). This proves that liposome tubes exist before the sample is prepared for TEM imaging.

The tube-like structures reported in both shear fields and sonicated liposomes are of various diameters, even in the micelle range. This may be attributed to the different shear

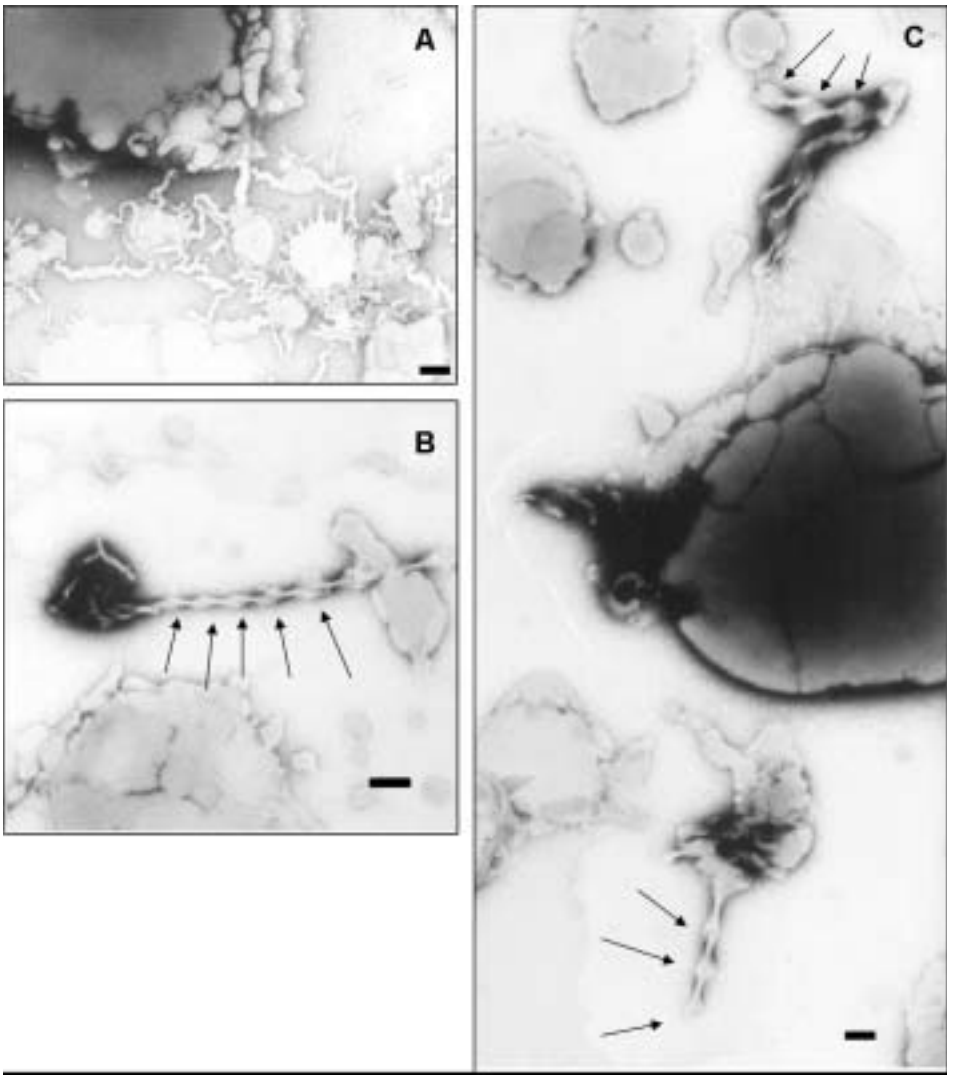

Figure 12. A. Electron micrograph of tube-like structures among sonicated liposomes. These liposomes contained 56 μg/mL of nystatin (although similar tubes were observed in nystatin-free liposomes). **B and C.** Evidence of "pinching-off" mechanism. In both **B** and **C** liposomes are shown with long undulating tube-like protrusions that appear to be pinching off to form smaller liposomes (arrows). Notice that the size of the forming liposome is on the order of 100 nm. These liposomes contained no nystatin. The length of the bar in all micrographs is 100 nm and were taken at ×17,000.

rates used (Cristini et al., 2003). We observe significant variability in tube diameter even within the same sample (Fig. 12). This may be due to the irregularities of the shear field surrounding cavitating microbubbles, the various sizes of such microbubbles, and the distance that the liposomes are located from the microbubble when pinch-off occurs. Also, lipid composition likely plays an important role in the length and diameter of these shear-induced tubes. As tubes form, specific types of lipid, originally present in the liposome membrane, may differentially partition into or out of the lipid tube based on curvature

constraints (Evans et al., 1987; Mukherjee et al., 1999). This could provide the lipid tubes with increased stability, which explains their presence many minutes after sonication. At the same time, as these tubes pinch off, the beta liposomes may develop a lipid mix that becomes resistant to tube formation, thus guaranteeing the long-term survival of beta liposomes, even in the presence of continued sonication.

While the pinch-off mechanism of colloids in a shear field has been well-defined, as well as the shear field produced by cavitation, there is little work connecting the two. Much investigation is still needed to verify this relationship. It should be possible to further test our hypothesis by using a mathematical model based on ultrasound parameters and the resultant shear field to predict liposome size and distribution. Changing ultrasound intensity or frequency would affect the strength of the shear field and perhaps the asymptotic liposome size observed. Successful production of liposomes with a desired size would prove useful in many biomedical, biophysics, and physical chemistry applications.

In conclusion, our goal was to meticulously characterize the size distribution of sonicated liposomes, and propose a model for their formation. We show that sonication can produce a fairly uniform population of smaller alpha liposomes, but a second population of beta liposomes remains even after 1h of bath sonication. Although the beta population may be small in number, it should not be disregarded. The presence of these larger liposomes will alter measurements dependent on total lipid and trapped volume.

Acknowledgments

We are deeply grateful to Drs. J. Walter Woodbury and W.G. Pitt for constructive comments on the manuscript and to Dr. Pitt for lending us the hydrophone. We are grateful to William Bernt of Particle Characterization Laboratories for providing the carbon black sample and for helpful discussions on dynamic light scattering. This work was supported by NIH grant #MH50003 and by a student research grant from Brigham Young University.

Reference

Abkarian, M., Lartigue, C., Viallat, A. (2002). Tank treading and unbinding of deformable vesicles in shear flow: Determination of the lift force. *Phys Rev Lett* 88:068103.

Brandl, M., Bachmann, D., Dreschler, M., Bauer, K. (1993). Liposome preparation using high-pressure homogenizers. In: *Liposome Technology: Liposome Preparation and Related Techniques.* CRC Press, pp. 49–65.

Cristini, V., Guido, S., Alfani, A., Blawzdziewicz, J., Loewenberg, M. (2003). Drop breakup and fragment size distribution in shear flow. *J Rheol* 47:1283–1298.

Drechsler, M., Bachmann, D., Brandl, M. (1995). Atomic force microscopical investigation of air-dried liposome specimens: Evaluation of a shrinkage correction factor for electron microscopical size analysis. 4th Liposome Research Days Conference, Albert-Ludwigs-Universität Freiburg, 30.8.–2.9.

Egelhaaf, S.U., Wehrli, E., Muller, M., Adrian, M., Schurtenberger, P. (1996). Determination of the size distribution of lecithin liposomes: A comparative study using freeze fracture, cryoelectron microscopy and dynamic light scattering. *Journal of Microscopy-Oxford* 184:214–228.

Elder, S.A. (1959). Cavitation microstreaming. *The Journal of Acoustical Society of America* 31:54–64.

Epstein, H., Afergan, E., Moise, T., Richter, Y., Rudich, Y., Golomb, G. (2006). Number-concentration of nanoparticles in liposomal and polymeric multiparticulate preparations: Empirical and calculation methods. *Biomaterials* 27:651–659.

Evans, E., Needham, D. (1987). Physical-properties of surfactant bilayer-membranes – thermal transitions, elasticity, rigidity, cohesion, and colloidal interactions. *Journal of Physical Chemistry* 91:4219–4228.

Finer, E.G., Flook, A.G., Hauser, H. (1972). Mechanism of sonication of aqueous egg yolk lecithin dispersions and nature of the resultant particles. *Biochimica et Biophysica Acta* 260:49–58.

Finsy, R., Deriemaeker, L., Dejaeger, N., Sneyers, R., Vanderdeelen, J., Vandermeeren, P., Demeyere, H., Stonemasui, J., Haestier, A., Clauwaert, J., Dewispelaere, W., Gillioen, P., Steyfkens, S., Gelade, E. (1993). Particle sizing by photon-correlation spectroscopy. 4. Resolution of bimodals and comparison with other particle sizing methods. *Particle & Particle Systems Characterization* 10:118–128.

Franklin, M.J., Brusilow, W.S.A., Woodbury, D.J. (2004). Determination of proton flux and conductance at pH 6.8 through single F-o sectors from Escherichia coli. *Biophys J* 87:3594–3599.

Frantzen, C.B., Ingebrigtsen, L., Skar, M., Brandl, M. (2003). Assessing the accuracy of routine photon correlation spectroscopy analysis of heterogeneous size distributions. *AAPS PharmSciTech* 4:E36.

Fromherz, P., Ruppel, D. (1985). Lipid vesicle formation – the transition from open disks to closed shells. *Febs Letters* 179:155–159.

Fromherz, P.C.R. c. a. D. R. p. (1986). From discoid micelles to spherical vesicles. The concept of edge activity. *Faraday Discuss Chem Soc* 81:39–48.

Hindes, W.C. (1999). Moment distributions. In: *Aerosol Technology.* John Wiley & Sons Inc., pp. 84–88.

Huang, C. (1969). Studies on phosphatidylcholine vesicles. Formation and physical characteristics. *Biochemistry* 8:344–352.

Hunter, D.G., Frisken, B.J. (1998). Effect of extrusion pressure and lipid properties on the size and polydispersity of lipid vesicles. *Biophys J* 74:2996–3002.

Israelachvili, J.N. (1985). *Intermolecular and Surface Forces: With Applications to Colloidal and Biological Systems.* London: Academic Press.

Kim, S., Martin, G.M. (1981). Preparation of cell-size unilamellar liposomes with high captured volume and defined size distribution. *Biochimica et Biophysica Acta* 646:1–9.

Koppel, D.E. (1972). Analysis of macromolecular polydispersity in intensity correlation spectroscopy: The method of cumulants. *J Chem Phys* 57:4814–4820.

Korgel, B.A., van Zanten, J.H., Monbouquette, H.G. (1998). Vesicle size distributions measured by flow field-flow fractionation coupled with multiangle light scattering. *Biophys J* 74:3264–3272.

Kraus, M., Wintz, W., Seifert, U., Lipowsky, R. (1996). Fluid vesicles in shear flow. *Phys Rev Lett* 77:3685–3688.

Lasch, J., Weissig, V., Brandl, M. (2003). Preparation of liposomes. In: *Liposomes: A Practical Approach.* Oxford University Press, pp. 3–27.

Lasic, D.D. (1987). A general-model of vesicle formation. *Journal of Theoretical Biology* 124:35–41.

Lasic, D.D. (1988). The mechanism of vesicle formation. *Biochemical Journal* 256:1–11.

Lin, H.Y., Thomas, J.L. (2003). PEG-lipids and oligo(ethylene glycol) surfactants enhance the ultrasonic permeabilizability of liposomes. *Langmuir* 19:1098–1105.

Litzinger, D.C., Buiting, A.M.J., Vanrooijen, N., Huang, L. (1994). Effect of liposome size on the circulation time and intraorgan distribution of amphipathic poly(ethylene Glycol)-containing liposomes. *Biochimica et Biophysica Acta-Biomembranes* 1190:99–107.

Liu, D., Mori, A., Huang, L. (1992). Role of liposome size and RES blockade in controlling biodistribution and tumor uptake of GM1-containing liposomes. *Biochim Biophys Acta* 1104:95–101.

MacDonald, R.C., Macdonald, R.I., Menco, B.P.M., Takeshita, K., Subbarao, N.K., Hu, L.R. (1991). Small-volume extrusion apparatus for preparation of large, unilamellar vesicles. *Biochimica et Biophysica Acta* 1061:297–303.

Marmottant, P., Hilgenfeldt, S. (2003). Controlled vesicle deformation and lysis by single oscillating bubbles. *Nature* 423:153–156.

Maulucci, G., De Spirito, M., Arcovito, G., Boffi, F., Castellano, A.C., Briganti, G. (2005). Particle size distribution in DMPC vesicles solutions undergoing different sonication times. *Biophys J* 88:3545–3550.

Mendes, E., Narayanan, J., Oda, R., Kern, F., Candau, S.J. (1997). Shear-induced vesicle to wormlike micelle transition. *J Phys Chem B* 101:2256–2258.

Moreno-Bello, M., Bonilla-Marin, M., Gonzalez-Beltran, C. (1988). Distribution of pore sizes in black lipid membranes treated with nystatin. *Biochim Biophys Acta* 944:97–100.

Morrison, I.D., Grabowski, E.F., Herb, C.A. (1985). Improved techniques for particle-size determination by quasi-elastic light-scattering. *Langmuir* 1:496–501.

Mukherjee, S., Soe, T.T., Maxfield, F.R. (1999). Endocytic sorting of lipid analogues differing solely in the chemistry of their hydrophobic tails. *Journal of Cell Biology* 144:1271–1284.

Nyborg, W.L. (1968). Mechanisms for the nonthermal effects of sound. *J ACM* 44:1302–1309.

Nyborg, W.L. (1982). Ultraonic microstreaming and related phenomena. *British Journal of Cancer* 45:156–160.

Nyborg, W.L. (2001). Biological effects of ultrasound: Development of safety guidelines. Part II: General review. *Ultrasound Med Biol* 27:301–333.

Parente, R.A., Lentz, B.R. (1984). Phase-behavior of large unilamellar vesicles composed of synthetic phospholipids. *Biochemistry* 23:2353–2362.

Peter, B.J., Kent, H.M., Mills, I.G., Vallis, Y., Butler, P.J.G., Evans, P.R., McMahon, H. T. (2004). BAR domains as sensors of membrane curvature: The amphiphysin BAR structure. *Science* 303:495–499.

Pick, U. (1981). Liposomes with a large trapping capacity prepared by freesing and thawing of sonicated phospholipid mixtures. *Arch Biochem Biophys* 212:187–197.

Provencher, S.W. (1982). A constrained regularization method for inverting data represented by linear algebraic or integral equations. *Comput Phys Commun* 27:213–227.

Rovira-Bru, M., Thompson, D.H., Szleifer, I. (2002). Size and structure of spontaneously forming liposomes in lipid/PEG-lipid mixtures. *Biophys J* 83:2419–2439.

Shahidzadeh, N., Bonn, D., Aguerre-Chariol, O., Meunier, J. (1998). Large deformations of giant floppy vesicles in shear flow. *Physical Review Letters* 81:4268–4271.

Sundaram, J., Mellein, B.R., Mitragotri, S. (2003). An experimental and theoretical analysis of ultrasound-induced permeabilization of cell membranes. *Biophysical Journal* 84:3087–3101.

Szoka, F., Olson, F., Heath, T., Vail, W., Mayhew, E., Papahadjopoulos, D. (1980). Preparation of unilamellar liposomes of intermediate size (0.1–0.2um) by a combination of reverse phase evaporation and extrusion through polycarbonate membranes. *Biochim Biophys Acta* 601:559–571.

Tenchov, B.G., Yanev, T.K. (1986). Weibull distribution of particle sizes obtained by uniform random fragmentation. *Journal of Colloid and Interface Science* 111:1–7.

Tenchov, B.G., Yanev, T.K., Tihova, M.G., Koynova, R.D. (1985). A probability concept about size distributions of sonicated lipid vesicles. *Biochimica et Biophysica Acta* 816:122–130.

Weiner, B.B., Tscharnuter, W.W., Bernt, W. (2002). Characterizing ASTM carbon black reference materials using a disc centrifuge photosedimentometer. *J Disper Sci Technol* 23:671–678.

Williams, A.R., Hughes, D.E., Nyborg, W.L. (1970). Hemolysis near a transversely oscillating wire. *Science* 169:871–873.

Woodbury, D.J. (1989). Pure lipid vesicles can induce channel-like conductances in planar bilayers. *J Membrane Biol* 109:145–150.

Woodbury, D.J. (1999). Nystatin/ergosterol method for reconstituting ion channels into planar lipid bilayers. In: *Methods in Enzymology.* Academic Press, pp. 319–339.

Woodbury, D.J., Hall, J.E. (1988). Role of channels in the fusion of vesicles with a planar bilayer. *Biophys J* 54:1053–1063.

Woodbury, D.J., Miller, C. (1990). Nystatin-induced liposome fusion – a versatile approach to ion channel reconstitution into planar bilayers. *Biophys J* 58:833–839.

Zasadzinski, J.A. (1986). Transmission electron microscopy observations of sonication-induced changes in liposome structure. *Biophys J* 49:1119–1130.